Published in final edited form as:
Structure. 2012 September 5; 20(9): 1463–1469. doi:10.1016/j.str.2012.08.009.

Structure of the Pentameric Ligand-Gated Ion Channel GLIC Bound With Anesthetic Ketamine

Jianjun Pan[1,#], **Qiang Chen**[1,#], **Dan Willenbring**[1], **David Mowrey**[1,2], **Xiang-Peng Kong**[3], **Aina Cohen**[4], **Christopher B. Divito**[5], **Yan Xu**[1,6,7,*], and **Pei Tang**[1,2,7,*]

[1]Department of Anesthesiology, Biomedical Science Tower 3, 3501 Fifth Avenue, University of Pittsburgh School of Medicine, Pittsburgh, PA, 15260

[2]Department of Computational and System Biology, Biomedical Science Tower 3, 3501 Fifth Avenue, University of Pittsburgh School of Medicine, Pittsburgh, PA, 15260

[3]Department of Biochemistry, 550 First Avenue, MSB 329, New York University School of Medicine, New York, NY 10016

[4]Stanford Synchrotron Radiation Lightsource, 2575 Sand Hill Rd., MS: 99, Menlo Park, CA, 94025

[5]Department of Neurobiology, Biomedical Science Tower 3, 3501 Fifth Avenue, University of Pittsburgh School of Medicine, Pittsburgh, PA, 15260

[6]Department of Structural Biology, Biomedical Science Tower 3, 3501 Fifth Avenue, University of Pittsburgh School of Medicine, Pittsburgh, PA, 15260

[7]Department of Pharmacology and Chemical Biology, Biomedical Science Tower 3, 3501 Fifth Avenue, University of Pittsburgh School of Medicine, Pittsburgh, PA, 15260

SUMMARY

Pentameric ligand-gated ion channels (pLGICs) are targets of general anesthetics, but a structural understanding of anesthetic action on pLGICs remains elusive. GLIC, a prokaryotic pLGIC, can be inhibited by anesthetics, including ketamine. The ketamine concentration leading to half-maximal inhibition on GLIC (58 μM) is comparable to that on neuronal nicotinic acetylcholine receptors. A 2.99-Å resolution X-ray structure of GLIC bound with ketamine revealed ketamine binding to an inter-subunit cavity that partially overlaps with the homologous antagonist-binding site in pLGICs. The functional relevance of the identified ketamine site was highlighted by profound changes in GLIC activation upon cysteine substitution of the cavity-lining residue N152. The relevance is also evidenced by changes in ketamine inhibition upon the subsequent chemical

Corresponding Authors, Prof. Pei Tang, 2049 Biomedical Science Tower 3, 3501 Fifth Avenue, University of Pittsburgh School of Medicine, Pittsburgh, PA, 15260, tangp@anes.upmc.edu, Tel: 412-383-9798, Fax: 412-648-8998, Prof. Yan Xu, 2048 Biomedical Science Tower 3, 3501 Fifth Avenue, University of Pittsburgh School of Medicine, Pittsburgh, PA, 15260, xu2@pitt.edu; Tel: 412-648-9922, Fax: 412-648-8998.
[#]These authors contributed equally to the study

ACCESSION NUMBERS

Atomic coordinates and structure factors for the ketamine bound GLIC have been deposited in the Protein Data Bank (http://www.pdb.org) with the accession code 4F8H.

SUPPLEMENTAL INFORMATION

Supplemental Information includes five figures, one table, and references and can be found with this article online.

labeling of N152C. The results provide novel structural insight into the molecular recognition of ketamine and are valuable for understanding the actions of anesthetics and other allosteric modulators on pLGICs.

INTRODUCTION

Clinical application of general anesthetics is indispensable in modern medicine, but the molecular mechanisms of general anesthesia remain unclear. The complexity of plausible anesthetic targets and the lack of accurate structural information of these targets have hindered progress towards a mechanistic understanding. Among all the receptors involved in neuronal signal transduction, a family of pentameric ligand-gated ion channels (pLGICs) has been identified as targets for general anesthetics. Anesthetics often inhibit the agonist-activated current in the excitatory nicotinic acetylcholine receptors (nAChRs) or serotonin 5-HT_3 receptors, but potentiate the inhibitory glycine and $GABA_A$ receptors (Franks and Lieb, 1994; Hemmings et al., 2005). Although our understanding of general anesthetic modulation on these receptors has progressed dramatically in the last decade (Forman and Miller, 2011), it remains a formative challenge to resolve high-resolution structures of these pLGICs, and to pinpoint where and how anesthetics act on these channels to modulate their functions.

The structure of a bacterial homologue of pLGICs from *Gloeobacter violaceus* (GLIC) has been solved by X-ray crystallography (Bocquet et al., 2009; Hilf and Dutzler, 2009), showing a similar architecture of extracellular (EC) and transmembrane domains (TM) to that of the *Torpedo marmorata* nAChR solved by electron microscopy (Unwin, 2005). The EC domain of GLIC resembles the X-ray structures of the acetylcholine-binding proteins (AChBPs) (Brejc et al., 2001; Celie et al., 2004; Hansen et al., 2005) and the EC domain of α1-nAChR (Dellisanti et al., 2007), presenting similar inter-subunit cavities for agonist or antagonist binding (Hansen et al., 2005). Despite the fact that GLIC opens upon lowering pH (Bocquet et al., 2007) and does not require agonist binding to the conventional site as for pLGICs, its responses to general anesthetics resemble those of nAChRs. A proton-activated Na^+ current in GLIC can be inhibited by anesthetics, as demonstrated previously (Nury et al., 2011; Weng et al., 2010) and in this study. Anesthetic binding sites in GLIC have been investigated by steady-state fluorescence quenching experiments (Chen et al., 2010) and X-ray crystallography (Nury et al., 2011). While the crystal structures of anesthetic desflurane- and propofol-bound GLIC revealed an intra-subunit binding site in the TM domain, the fluorescence experiments with halothane and thiopental suggested additional sites in the EC and TM domains of GLIC. The sensitivity to anesthetics and amenability to crystal structure determination make GLIC ideally suited for revealing where and how general anesthetics act on pLGICs.

Ketamine has been widely used for the induction and maintenance of general anesthesia. Although ketamine is commonly known as a dissociative anesthetic acting as a noncompetitive antagonist on the N-methyl-D-aspartate (NMDA) receptor (Harrison and Simmonds, 1985), it is also a potent inhibitor of neuronal nAChRs (Coates and Flood, 2001; Yamakura et al., 2000). The action sites of ketamine in these receptors have not been identified previously. Here we show for the first time the crystal structure of ketamine-bound GLIC. A preexisting cavity in the EC domain of GLIC is found to be the site for ketamine binding. Functional relevance of the site is evidenced by electrophysiology measurements in combination with site-directed mutations and subsequent chemical labeling to mimic anesthetic binding. Combined with the previous knowledge of anesthetic binding to the TM domain of GLIC (Nury et al., 2011), the newly discovered anesthetic binding site in the EC domain provides an additional structural template for the future design and evaluation of novel general anesthetics and therapeutic allosteric modulators of pLGICs.

RESULTS

Ketamine inhibition on GLIC

We found that the anesthetic ketamine inhibited currents of the *Xenopus oocytes* expressing GLIC in a concentration-dependent manner (Fig. 1). At the proton concentration near EC20 (pH 5.5) for GLIC activation, inhibition concentration with half-maximal response (IC50) for ketamine on GLIC is 58 μM, which is comparable to the ketamine IC50 values on the α7 nAChR (20 μM) and the α4β2 nAChR (50–72 μM) (Coates and Flood, 2001; Yamakura et al., 2000).

The crystal structure of ketamine-bound GLIC

To identify ketamine binding site(s) in GLIC, we co-crystallized ketamine with GLIC and solved the structure to a resolution of 2.99 Å. Crystallographic and refinement parameters are summarized in Table 1. Strong electron densities for ketamine were found in all five equivalent pockets in the Fo-Fc omit electron density map (Fig. S1). Fig. 2 shows the refined structure and a stereo view of the 2Fo-Fc electron density map for the ketamine binding site, revealing ketamine in a pre-existing cavity between adjacent subunits in the EC domain of GLIC. The ketamine site in GLIC is near the homologous orthosteric agonist site in Cys-loop receptors, but it is 9–10 Å closer the TM domain (Fig. S2). It partially overlaps with the binding interface of large antagonists in Cys-loop receptors (Bourne et al., 2010; Hansen et al., 2005).

Interactions stabilizing ketamine in the binding pocket

Positively charged at low pH, ketamine is stabilized in an amphipathic pocket, where it contacts mostly hydrophilic residues to form electrostatic interactions with these residues, in addition to van der Waals interactions with some hydrophobic residues. As depicted in Fig. 3, on one side of the pocket, the chloro group of ketamine points to the positively charged amine of K183 of β10 and the phenyl ring faces F174 and L176 of loop C. On a different side of the pocket, the aminium of ketamine makes electrostatic interactions with side chains of N152, D153, and D154 of the β8-β9 loop (loop F). The carbonyl group of ketamine can potentially form a hydrogen bond with the hydroxyl group of Y23 on β1. The amide carbonyl oxygen of N152 is 3 Å away from the aminium of ketamine. GLIC is activated at low pH and the protonation states of titratable residues are responsible for channel activities. K183 of the principal side carries a positive charge on its side chain whereas the side chains of D153 and D154 of the complementary side are likely negatively charged. Thus, electrostatic interactions have contributed significantly to stabilizing ketamine binding (Fig. S3).

Functional relevance of the ketamine-binding pocket

The functional relevance of the identified ketamine site was validated by site-directed mutations and subsequent chemical labeling of a pocket residue to mimic anesthetic binding. As shown in Fig. 4, the ketamine binding pocket is involved in the GLIC activation. A single mutation in the pocket, N152C, shifted EC50 from pH 5.0 in the wild type (wt) GLIC to pH 5.4 in the N152C mutant (Fig. 4a). Ketamine binding to the pocket is evidenced by a higher IC50 value for the N152C mutant (110 μM) in comparison to IC50 of the wt GLIC (58 μM) (Fig. 4b). Removal of a favorable electrostatic interaction between the aminium of ketamine and the amide carbonyl oxygen of N152 in the mutant may account for the reduced ketamine inhibition. The functional relevance of the ketamine binding site is further substantiated by the results of labeling 8-(chloromercuri)-2-dibenzofuransulfonic acid (CBFS) to N152C after mutating the only native cysteine residue in GLIC (C27A). Covalent labeling of the introduced cysteines with reagents like CBFS has been used previously to

mimic alcohol binding to specific residues in pLGICs (Howard et al., 2011). The CBFS bonding to N152C mimicked the ketamine effect and resulted in inhibition to the mutant current (Fig. 4c). The residual current from the CBFS bonding could be completely inhibited by ketamine, but with a higher IC50 of 180 μM (Fig. S4). The weakening of ketamine's inhibition is somewhat expected, considering the interruption of CBFS to the pocket and to potential interactions between ketamine and its surrounding residues. The channel resumed a normal function once CBFS was removed from N152C after treatment with 10 mM DTT. Collectively, these data indisputably demonstrate functional significance of the ketamine-binding pocket revealed in the crystal structure.

DISCUSSION

The functional importance of the EC domain in pLGICs has been well established based on the data that agonist or antagonist binding to the orthosteric site regulates channel activities allosterically (Changeux and Edelstein, 2005; Sine and Engel, 2006). Our structure reveals a drug-binding pocket in the EC domain, showing that ketamine is not in, but 9–10 Å below, the orthosteric agonist-binding site. In the superimposed crystal structures of the ketamine-bound GLIC and the agonist- or antagonist-bound AChBP (Bourne et al., 2010; Celie et al., 2004; Hansen et al., 2005; Hibbs et al., 2009; Ihara et al., 2008; Talley et al., 2008), one can see clearly that ketamine is outside the binding loci for agonists (Fig. S2). However, the ketamine binding site overlaps partially with the extended interaction surface of bulky antagonists bound to AChBP (Fig. S2), suggesting that ketamine may inhibit GLIC in the way similar to that competitive antagonists inhibit the functions of nAChRs. No agonist other than protons has been found for GLIC so far. It is unclear if the EC domain, especially the region for agonist or antagonist binding, plays any functional role in GLIC as in other pLGICs. Our data highlight the functional importance of the EC domain of GLIC. The functional relevance of the identified ketamine site has been established by compelling data of mutations and the CBFS labeling in combination with electrophysiology measurements. Several residues lining the ketamine pocket in GLIC are from the β8-β9 loop and β10. Their interplay with the TM2-TM3 loop from the channel domain is thought to be essential for communication between agonist binding and channel activation in pLGICs (Sine and Engel, 2006). Both our structural and functional results suggest that the pre-existing cavity in the EC domain, other than the conventional agonist-binding site, can accommodate a drug molecule and modulate the functions of GLIC channel.

Despite a profound inhibition effect on GLIC upon ketamine binding, our crystal structure shows little difference from the apo GLIC structure (Bocquet et al., 2009; Hilf and Dutzler, 2009). For residues within 4 Å from the bound ketamine, their root mean square deviation (RMSD) relative to the apo structure is only 0.4 Å. The structural resilience to anesthetic binding was also observed in the desflurane- and propofol-bound GLIC structures (Nury et al., 2011). Whether a structural response to ligand binding can be observed under crystallization may depend on binding sites, ligands, crystallization conditions, or other factors. The crystal structure of ELIC, the pentameric ligand-gated ion channel from *Erwinia chrysanthemi*, shows significant conformational changes near and beyond the binding site of acetylcholine (Pan et al., 2012), while agonist binding to the homologous site of the pentameric *Caenorhabditis elegans* glutamate-gated chloride channel alpha (GluCl) results in little conformational changes in the crystal structures (Hibbs and Gouaux, 2011). It remains a challenge to capture different conformations crystallographically for a given pLGIC (Gonzalez-Gutierrez et al., 2012).

The structural and functional results of ketamine binding to GLIC present a compelling case for the allosteric action of anesthetics. The ketamine pocket is nearly 30 Å away from the channel gate. The previously identified site for propofol or desflurane is in the upper part of

the TM domain within a subunit of GLIC (Nury et al., 2011), distinct from the ketamine binding site. Two factors may have contributed to different sites of allosteric action for these drugs. First, ketamine is more soluble in the aqueous phase than propofol and desflurane. It is more attractive to the solvent-exposed pocket offering electrostatic, hydrogen bonding, and van de Waals interactions (Fig. S3). Second, ketamine has a larger molecular size than either propofol or desflurane. The ketamine pocket in GLIC is comprised of flexible loops and has a volume of ~ 248 $Å^3$, compatible with a ketamine volume of 219 $Å^3$ (Table S1). Crystal structures of anesthetic bound GLIC reported here and previously (Nury et al., 2011) reveal at least two sets of sites for anesthetic binding. Existence of multiple anesthetic binding sites in GLIC has been suggested by several studies. Tryptophan fluorescence quenching experiments showed halothane and thiopental binding in the EC domain, TM domain, and the EC-TM interface of GLIC (Chen et al., 2010). Molecular dynamic simulations suggested that in addition to EC and TM domains, isoflurane could also migrate into the GLIC channel (Brannigan et al., 2010; Willenbring et al., 2011). Multiple anesthetic sites were also identified in other pLGICs. In *Torpedo* nAChR, azietomidate was photolabeled not only to some pore-ling residues, but also to the agonist-binding site in the EC domain (Ziebell et al., 2004). The volatile anesthetic halothane was also found to be photolabeled to both the TM and EC domains (Chiara et al., 2003). Some halothane-labeled residues in the EC domain of nAChR were from the β9 and β10 strands (Chiara et al., 2003), suggesting that the ketamine site in our structure represents a homologous site for anesthetic binding in other pLGICs.

Ketamine has been traditionally classified as an NMDA receptor antagonist (Harrison and Simmonds, 1985). Our structural and functional data reported here, along with previous functional studies of ketamine on nAChRs, may aid in a paradigm shift and call for a comprehensive examination of ketamine action on pLGICs. Ketamine inhibited the recombinant neuronal nAChRs in a subunit-dependent manner (Coates and Flood, 2001; Yamakura et al., 2000). IC_{50} values of ketamine measured from *Xenopus oocyte* expressing human α7 and α4β2 nAChRs (Coates and Flood, 2001; Yamakura et al., 2000) were close to our measured value with GLIC in this study. From the modeled structures of the α7 and α4β2 nAChRs (Haddadian et al., 2008; Mowrey et al., 2010), it is notable that both proteins have a pocket similar to the ketamine pocket in GLIC, where several acidic residues are on one side of the pocket (Fig. S5). These negatively charged residues could attract ketamine and stabilize the ketamine binding. A greater number of negatively charged residues in the pocket of α7 than α4β2 nAChRs seem to be consistent with the observation that the α7 nAChR is more sensitive to ketamine inhibition than the α4β2 nAChR (Coates and Flood, 2001).

The discovery of the ketamine-binding pocket expands the scope of the drug-binding mode and is particularly valuable for the understanding of functional data related to drug action in the EC domain of pLGICs. There may also be other sites for ligand binding in the EC domain of heteromeric nAChRs and $GABA_A$ receptors (Hansen and Taylor, 2007). For a long time, the search for targets of soluble drugs, such as benzodiazepine and its derivatives, was focused on sites equivalent to but not the orthosteric ligand site in $GABA_A$ receptors (Boileau et al., 1998; Morlock and Czajkowski, 2011; Sigel and Buhr, 1997). Residue selection for mutagenesis and subsequent functional studies have relied heavily on structures of ligand-bound AChBPs (Celie et al., 2004; Hansen et al., 2005), due to the limited number of high-resolution structures with ligand binding to pLGICs (Dellisanti et al., 2007; Li et al., 2011; Pan et al., 2012) and the lack of experimental structures for $GABA_A$ receptors. The atomic binding mode of ketamine in GLIC provides an additional structural template, which is invaluable for the design of novel modulators or the search for optimal binding modes of benzodiazepine derivatives at the interfaces of various subtype subunits (Richter et al., 2012).

EXPERIMENTAL PROCEDURES

Protein expression and purification

GLIC was expressed as a fusion of Maltose-binding protein (MBP) using a plasmid generously provided by Professor Raimund Dutzler's group. The protocol for GLIC expression and purification was modified from the published protocols (Bocquet et al., 2009; Hilf and Dutzler, 2009) and detailed in the online supplemental materials. The purified GLIC was concentrated to ~10 mg/ml and used for crystallization.

Crystallization

Crystallization was performed using the sitting-drop method at 4°C. GLIC was pre-equilibrated with 0.5 mg/mL *E. coli* polar lipids (Avanti Polar Lipids) and 1 mM ketamine (Fort Dodge, IA) for at least one hour at 4°C before being mixed in a 1:1 ratio with the reservoir solution containing 10–12% PEG 4000, 225 mM ammonium sulfate, and 50 mM sodium acetate buffer (pH 3.9 – 4.1). Crystals of GLIC containing ketamine usually appeared within one week. For cryo-protection, the crystals were flash frozen in liquid nitrogen after socking for 30 mins in the reservoir solution supplemented with 20% glycerol and 10 mM ketamine.

Structural data collection and analysis

The X-ray diffraction data were acquired on beamline 12-2 at the Stanford Synchrotron Radiation Lightsource and processed using the XDS program (Kabsch, 2010). The structure was determined by molecular replacement using the apo-GLIC structure (PDB code 3EAM) without detergent, lipid, and water molecules, as the starting model. Phenix (version: 1.6.4-486) (Adams et al., 2010) and COOT (Emsley et al., 2010) were used for structure refinement and model building. After several cycles of refinement, six detergent and ten lipid molecules were built into well-defined extra electron densities using COOT (Emsley et al., 2010). Non-crystallographic symmetry (NCS) restraints were applied for five subunits in each unit cell. Automatic solvent detection, update, and refinement were used for the placement of water molecules. Manual inspection and adjustment were performed at a later stage. Finally, ketamine binding sites were determined based on the Fo-Fc difference map and ketamine molecules were built into five equivalent sites showing significant electron densities. Initial ketamine geometry was obtained using Gaussian 03 at the HF/6-31G level of theory (Frisch et al., 2003). Both *R*- and *S*-ketamine enantiomers were used in structural refinements. R-ketamine showed interactions with surrounding residues more energetically favorable and was used in the final structure. The final structure was obtained after additional refinement cycles. Crystal structure analysis was performed using Phenix and CCP4 (Winn et al., 2011). PyMOL (Schrodinger, 2010) and VMD (Humphrey et al., 1996) programs were used for structural analysis and figure preparation.

Molecular biology and GLIC expression in Xenopus laevis oocytes

Plasmids encoding GLIC in the pTLN vector for GLIC expression in *Xenopus laevis* oocytes was a generous gift from Professor Raimund Dutzler of University of Zürich, Zürich, Switzerland. Site-directed mutagenesis was introduced with the QuikChange Lightning Kit (Stratagene, Santa Clara, CA) and conformed by sequencing. The plasmid DNA was linearized with MluI enzyme (New England BioLabs, Ipswich, MA). Capped complementary RNA was transcribed with the mMessage mMachine SP6 kit (Ambion, Austin, TX) and purified with the RNeasy kit (Qiagen, Valencia, CA). The defolliculated stage V-VI oocytes were injected with cRNA (10–25 ng/each) and maintained at 18°C in Modified Barth's Solution (MBS) containing 88 mM NaCl, 1 mM KCl, 2.4 mM $NaHCO_3$, 15 mM HEPES, 0.3 mM $Ca(NO_3)_2$, 0.41 mM $CaCl_2$, 0.82 mM $MgSO_4$, 10 μg/ml sodium

penicillin, 10 μg/ml streptomycin sulphate, 100 μg/ml gentamycin sulphate, pH 6.7. Functional measurements were performed on oocytes 16–40 hours after the injection.

Oocyte Electrophysiology

Two-electrode voltage clamp experiments were performed at room temperature with a model OC-725C amplifier (Warner Instruments) and a 20-μl oocyte recording chamber (Automate Scientific). Oocytes were perfused with ND96 buffer (96 mM NaCl, 2 mM KCl, 1.8 mM $CaCl_2$, 1 mM $MgCl_2$, 5 mM HEPES, pH7.4) and clamped to a holding potential of −40 to −60 mV. Data were collected and processed using Clampex 10 (Molecular Devices). Non-linear regressions were performed using Prism software (Graphpad). Ketamine (Sigma-Aldrich Inc, St. Louis, MO) was prepared as a 100 mM stock at a specific pH and diluted with freshly prepared ND96 to a desired concentration. 8-(chloromercuri)-2-dibenzofuransulfonic acid (CBFS) was purchased as sodium salt (Sigma-Aldrich Inc, St. Louis, MO). The stock solution of CBFS (200 μM) was prepared with ND96 and diluted to a desired concentration before application. To measure CBFS labeling effects, data were collected at various pH or various ketamine concentrations at pEC20; followed by ~2-min washout using ND96 (pH 7.4); 1–2 minutes treatment with 20 μl CBFS; ~ 2 minutes to washout free CBFS; data collection at various pH or various ketamine concentrations at a new pEC20. Covalent bonding of CBFS to GLIC mutants was confirmed by comparing currents at pEC20 before and after applying the reducing reagent, 10 mM dithiothreitol (DTT), to the CBFS-treated oocytes.

Supplementary Material

Refer to Web version on PubMed Central for supplementary material.

Acknowledgments

We thank Prof. Raimund Dutzler's lab for the GLIC plasmid and the discussion about GLIC expression; Prof. Thomas R. Kleyman's lab for providing *Xenopus laevis oocytes* for the electrophysiology experiments; Prof. Ossama B. Kashlan and Dr. Tommy Tillman for their help in functional measurements; Profs. Ken Yoshida, Susan Amara, Guillermo Calero and Mr. Jared Sampson for their assistance in the early stage of the project; Ms. Sandra C. Hirsch for her editorial assistance. Portions of this research were carried out at the Stanford Synchrotron Radiation Lightsource, a Directorate of SLAC National Accelerator Laboratory and an Office of Science User Facility operated for the U.S. Department of Energy Office of Science by Stanford University. The SSRL Structural Molecular Biology Program is supported by the DOE Office of Biological and Environmental Research, and by the National Institutes of Health, National Institute of General Medical Sciences (including P41GM103393) and the National Center for Research Resources (P41RR001209). The research was supported by NIH grants R01GM066358, R01GM056257, R37GM049202, and T32GM075770.

REFERENCES

Adams PD, Afonine PV, Bunkoczi G, Chen VB, Davis IW, Echols N, Headd JJ, Hung LW, Kapral GJ, Grosse-Kunstleve RW, et al. PHENIX: a comprehensive Python-based system for macromolecular structure solution. Acta Crystallogr. D Biol. Crystallogr. 2010; 66:213–221. [PubMed: 20124702]

Bocquet N, Nury H, Baaden M, Le Poupon C, Changeux JP, Delarue M, Corringer PJ. X-ray structure of a pentameric ligand-gated ion channel in an apparently open conformation. Nature. 2009; 457:111–114. [PubMed: 18987633]

Bocquet N, Prado de Carvalho L, Cartaud J, Neyton J, Le Poupon C, Taly A, Grutter T, Changeux JP, Corringer PJ. A prokaryotic proton-gated ion channel from the nicotinic acetylcholine receptor family. Nature. 2007; 445:116–119. [PubMed: 17167423]

Boileau AJ, Kucken AM, Evers AR, Czajkowski C. Molecular dissection of benzodiazepine binding and allosteric coupling using chimeric gamma-aminobutyric acidA receptor subunits. Mol. Pharmacol. 1998; 53:295–303. [PubMed: 9463488]

Bourne Y, Radic Z, Araoz R, Talley TT, Benoit E, Servent D, Taylor P, Molgo J, Marchot P. Structural determinants in phycotoxins and AChBP conferring high affinity binding and nicotinic AChR antagonism. Proc. Natl. Acad. Sci. USA. 2010; 107:6076–6081. [PubMed: 20224036]

Brannigan G, LeBard DN, Henin J, Eckenhoff RG, Klein ML. Multiple binding sites for the general anesthetic isoflurane identified in the nicotinic acetylcholine receptor transmembrane domain. Proc. Natl. Acad. Sci. USA. 2010; 107:14122–14127. [PubMed: 20660787]

Brejc K, van Dijk WJ, Klaassen RV, Schuurmans M, van Der Oost J, Smit AB, Sixma TK. Crystal structure of an ACh-binding protein reveals the ligand-binding domain of nicotinic receptors. Nature. 2001; 411:269–276. [PubMed: 11357122]

Celie PH, van Rossum-Fikkert SE, van Dijk WJ, Brejc K, Smit AB, Sixma TK. Nicotine and carbamylcholine binding to nicotinic acetylcholine receptors as studied in AChBP crystal structures. Neuron. 2004; 41:907–914. [PubMed: 15046723]

Changeux JP, Edelstein SJ. Allosteric mechanisms of signal transduction. Science. 2005; 308:1424–1428. [PubMed: 15933191]

Chen Q, Cheng MH, Xu Y, Tang P. Anesthetic binding in a pentameric ligandgated ion channel: GLIC. Biophys. J. 2010; 99:1801–1809. [PubMed: 20858424]

Chiara DC, Dangott LJ, Eckenhoff RG, Cohen JB. Identification of nicotinic acetylcholine receptor amino acids photolabeled by the volatile anesthetic halothane. Biochemistry. 2003; 42:13457–13467. [PubMed: 14621991]

Coates KM, Flood P. Ketamine and its preservative, benzethonium chloride, both inhibit human recombinant alpha7 and alpha4beta2 neuronal nicotinic acetylcholine receptors in Xenopus oocytes. Br. J. Pharmacol. 2001; 134:871–879. [PubMed: 11606328]

Dellisanti CD, Yao Y, Stroud JC, Wang ZZ, Chen L. Crystal structure of the extracellular domain of nAChR alpha1 bound to alpha-bungarotoxin at 1.94 A resolution. Nat. Neurosci. 2007; 10:953–962. [PubMed: 17643119]

Emsley P, Lohkamp B, Scott WG, Cowtan K. Features and development of Coot. Acta Crystallogr. D Biol. Crystallogr. 2010; 66:486–501. [PubMed: 20383002]

Forman SA, Miller KW. Anesthetic sites and allosteric mechanisms of action on Cys-loop ligand-gated ion channels. Can. J. Anaesth. 2011; 58:191–205. [PubMed: 21213095]

Franks NP, Lieb WR. Molecular and cellular mechanisms of general anaesthesia. Nature. 1994; 367:607–614. [PubMed: 7509043]

Frisch, MJ.; Trucks, GW.; Schlegel, HB.; Scuseria, GE.; Robb, MA.; Cheeseman, JR.; Montgomery, JA.; Vreven, T.; Kudin, KN.; Burant, JC., et al. Gaussian 03, Revision C.02. 2003.

Gonzalez-Gutierrez G, Lukk T, Agarwal V, Papke D, Nair SK, Grosman C. Mutations that stabilize the open state of the Erwinia chrisanthemi ligand-gated ion channel fail to change the conformation of the pore domain in crystals. Proc. Natl. Acad. Sci. USA. 2012; 109:6331–6336. [PubMed: 22474383]

Haddadian EJ, Cheng MH, Coalson RD, Xu Y, Tang P. In silico models for the human alpha4beta2 nicotinic acetylcholine receptor. J. Phys. Chem. B. 2008; 112:13981–13990. [PubMed: 18847252]

Hansen SB, Sulzenbacher G, Huxford T, Marchot P, Taylor P, Bourne Y. Structures of Aplysia AChBP complexes with nicotinic agonists and antagonists reveal distinctive binding interfaces and conformations. EMBO J. 2005; 24:3635–3646. [PubMed: 16193063]

Hansen SB, Taylor P. Galanthamine and non-competitive inhibitor binding to ACh-binding protein: evidence for a binding site on non-alpha-subunit interfaces of heteromeric neuronal nicotinic receptors. J. Mol. Biol. 2007; 369:895–901. [PubMed: 17481657]

Harrison NL, Simmonds MA. Quantitative studies on some antagonists of Nmethyl D-aspartate in slices of rat cerebral cortex. Br. J. Pharmacol. 1985; 84:381–391. [PubMed: 2858237]

Hemmings HC Jr, Akabas MH, Goldstein PA, Trudell JR, Orser BA, Harrison NL. Emerging molecular mechanisms of general anesthetic action. Trends Pharmacol. Sci. 2005; 26:503–510. [PubMed: 16126282]

Hibbs RE, Gouaux E. Principles of activation and permeation in an anionselective Cys-loop receptor. Nature. 2011; 474:54–60. [PubMed: 21572436]

Hibbs RE, Sulzenbacher G, Shi J, Talley TT, Conrod S, Kem WR, Taylor P, Marchot P, Bourne Y. Structural determinants for interaction of partial agonists with acetylcholine binding protein and

neuronal alpha7 nicotinic acetylcholine receptor. EMBO. J. 2009; 28:3040–3051. [PubMed: 19696737]

Hilf RJ, Dutzler R. Structure of a potentially open state of a proton-activated pentameric ligand-gated ion channel. Nature. 2009; 457:115–118. [PubMed: 18987630]

Howard RJ, Murail S, Ondricek KE, Corringer PJ, Lindahl E, Trudell JR, Harris RA. Structural basis for alcohol modulation of a pentameric ligand-gated ion channel. Proc. Natl. Acad. Sci. USA. 2011; 108:12149–12154. [PubMed: 21730162]

Humphrey W, Dalke A, Schulten K. VMD: visual molecular dynamics. J. Mol. Graph. 1996; 14:33–38. 27–38. [PubMed: 8744570]

Ihara M, Okajima T, Yamashita A, Oda T, Hirata K, Nishiwaki H, Morimoto T, Akamatsu M, Ashikawa Y, Kuroda S, et al. Crystal structures of Lymnaea stagnalis AChBP in complex with neonicotinoid insecticides imidacloprid and clothianidin. Invert. Neurosci. 2008; 8:71–81. [PubMed: 18338186]

Kabsch W. Integration, scaling, space-group assignment and post-refinement. Acta Crystallogr. D Biol. Crystallogr. 2010; 66:133–144. [PubMed: 20124693]

Li SX, Huang S, Bren N, Noridomi K, Dellisanti CD, Sine SM, Chen L. Ligand-binding domain of an alpha(7)-nicotinic receptor chimera and its complex with agonist. Nat. Neurosci. 2011; 14:1253–1259. [PubMed: 21909087]

Morlock EV, Czajkowski C. Different residues in the GABAA receptor benzodiazepine binding pocket mediate benzodiazepine efficacy and binding. Mol. Pharmacol. 2011; 80:14–22. [PubMed: 21447642]

Mowrey D, Haddadian EJ, Liu LT, Willenbring D, Xu Y, Tang P. Unresponsive correlated motion in alpha7 nAChR to halothane binding explains its functional insensitivity to volatile anesthetics. J. Phys. Chem. B. 2010; 114:7649–7655. [PubMed: 20465243]

Nury H, Van Renterghem C, Weng Y, Tran A, Baaden M, Dufresne V, Changeux JP, Sonner JM, Delarue M, Corringer PJ. X-ray structures of general anaesthetics bound to a pentameric ligand-gated ion channel. Nature. 2011; 469:428–431. [PubMed: 21248852]

Pan J, Chen Q, Willenbring D, Yoshida K, Tillman T, Kashlan OB, Cohen A, Kong XP, Xu Y, Tang P. Structure of the pentameric ligand-gated ion channel ELIC cocrystallized with its competitive antagonist acetylcholine. Nat. Commun. 2012; 3:714. [PubMed: 22395605]

Richter L, de Graaf C, Sieghart W, Varagic Z, Morzinger M, de Esch IJ, Ecker GF, Ernst M. Diazepam-bound GABA(A) receptor models identify new benzodiazepine binding-site ligands. Nat. Chem. Biol. 2012; 8:455–464. [PubMed: 22446838]

Schrodinger, L. The PyMOL Molecular Graphics System, Version 1.3r1. 2010.

Sigel E, Buhr A. The benzodiazepine binding site of GABAA receptors. Trends Pharmacol. Sci. 1997; 18:425–429. [PubMed: 9426470]

Sine SM, Engel AG. Recent advances in Cys-loop receptor structure and function. Nature. 2006; 440:448–455. [PubMed: 16554804]

Talley TT, Harel M, Hibbs RE, Radic Z, Tomizawa M, Casida JE, Taylor P. Atomic interactions of neonicotinoid agonists with AChBP: molecular recognition of the distinctive electronegative pharmacophore. Proc. Natl. Acad. Sci. USA. 2008; 105:7606–7611. [PubMed: 18477694]

Unwin N. Refined structure of the nicotinic acetylcholine receptor at 4A resolution. J. Mol. Biol. 2005; 346:967–989. [PubMed: 15701510]

Weng Y, Yang L, Corringer PJ, Sonner JM. Anesthetic sensitivity of the Gloeobacter violaceus proton-gated ion channel. Anesth. Analg. 2010; 110:59–63. [PubMed: 19933531]

Willenbring D, Tian Liu L, Xu Y, Tang P. Binding of Isoflurane to Glic Alters the Structure and Dynamics of the Protein. Biophys. J. 2011; 100:273a.

Winn MD, Ballard CC, Cowtan KD, Dodson EJ, Emsley P, Evans PR, Keegan RM, Krissinel EB, Leslie AG, McCoy A, et al. Overview of the CCP4 suite and current developments. Acta Crystallogr. D Biol. Crystallogr. 2011; 67:235–242. [PubMed: 21460441]

Yamakura T, Chavez-Noriega LE, Harris RA. Subunit-dependent inhibition of human neuronal nicotinic acetylcholine receptors and other ligand-gated ion channels by dissociative anesthetics ketamine and dizocilpine. Anesthesiology. 2000; 92:1144–1153. [PubMed: 10754635]

Ziebell MR, Nirthanan S, Husain SS, Miller KW, Cohen JB. Identification of binding sites in the nicotinic acetylcholine receptor for [3H]azietomidate, a photoactivatable general anesthetic. J. Biol. Chem. 2004; 279:17640–17649. [PubMed: 14761946]

Highlights

- The structure of ketamine-bound GLIC reveals a novel anesthetic binding site
- The study provides compelling evidence for allosteric inhibition by anesthetics
- Ketamine inhibition on GLIC is similar to competitive antagonist action on nAChRs
- Ketamine directly acts on pLGICs in addition to NMDA receptors

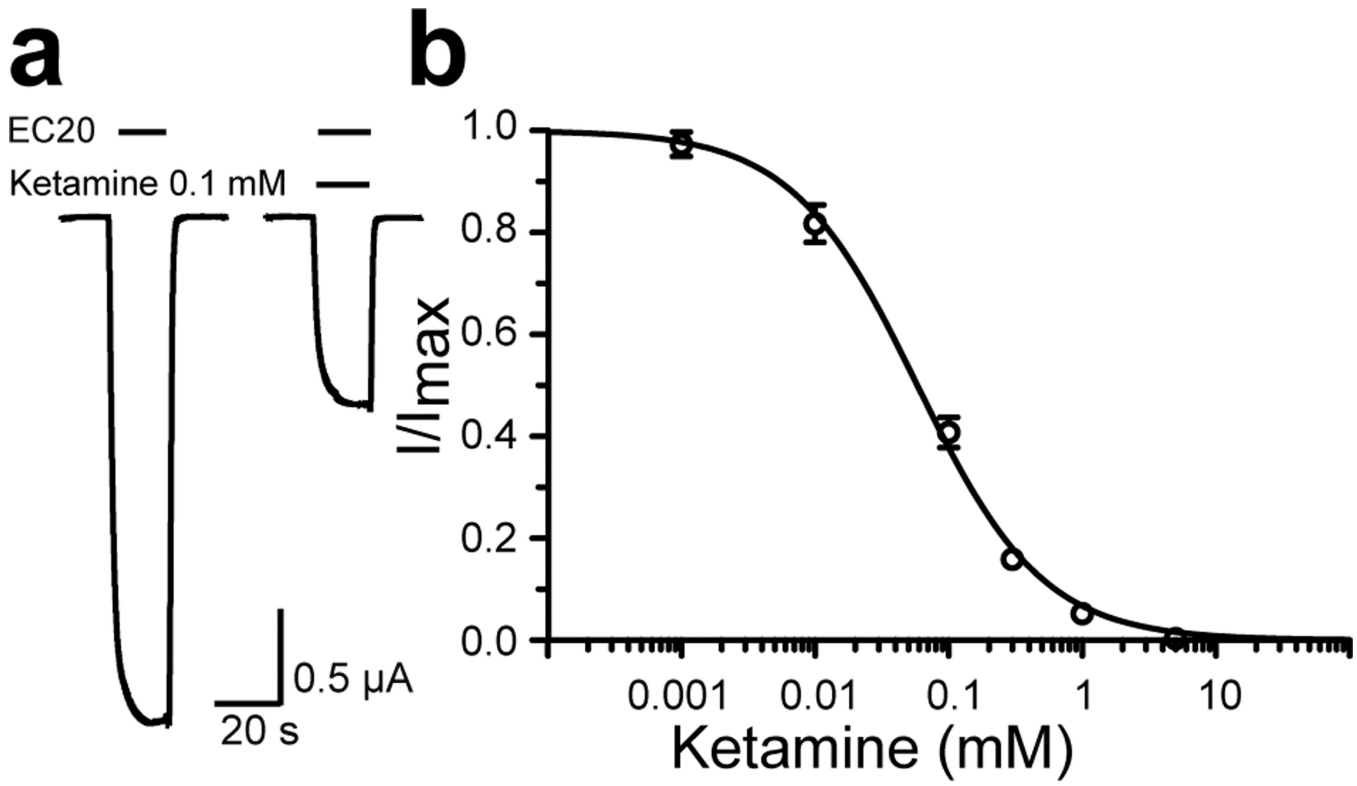

Figure 1. Ketamine inhibition of GLIC at EC20

(a) Representative current traces of GLIC expressed in *Xenopus oocytes* in the absence and presence of 100 μM ketamine. (**b**) Inhibition of the GLIC current by ketamine. Response to inhibition is expressed as a fraction of current induced at EC20 in the presence of an indicated concentration of ketamine relative to that in the absence of ketamine. The data are reported as the mean ± SEM from n ≥ 8 oocytes and fit to the Hill equation. Error bars less than the symbol size are not visible.

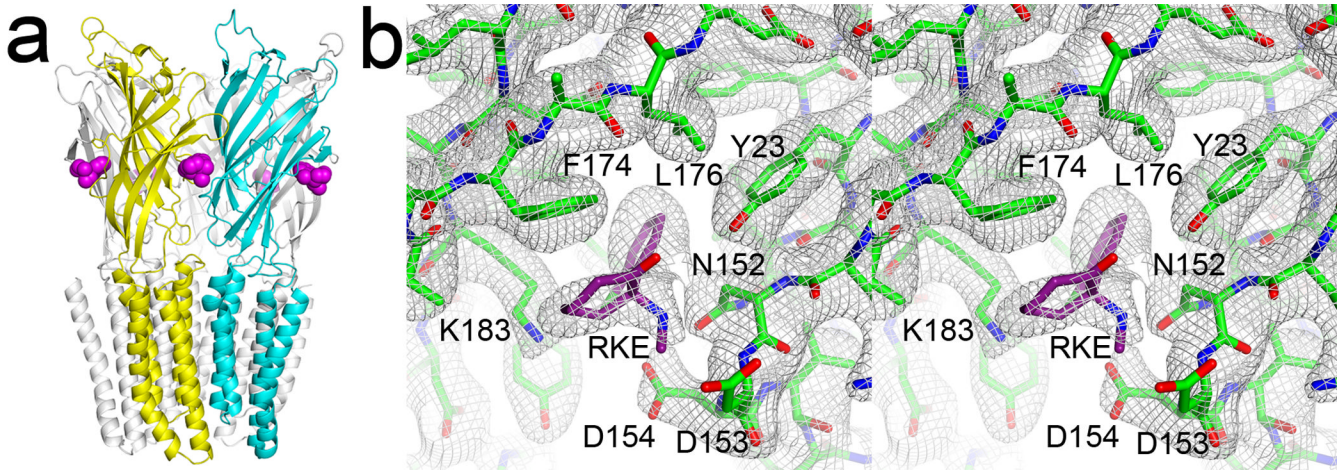

Figure 2. The crystal structure of GLIC bound with five ketamine molecules

(**a**) A side view of the structure with ketamine molecules in purple color. A pair of principal and complementary subunits for ketamine binding is depicted in yellow and cyan, respectively. Note that ketamine is a few Å below loop C. (**b**) A stereo view of the 2Fo-Fc electron density map, contoured at 1.0 σ level, for the ketamine binding site. See also Figures S1 and S2.

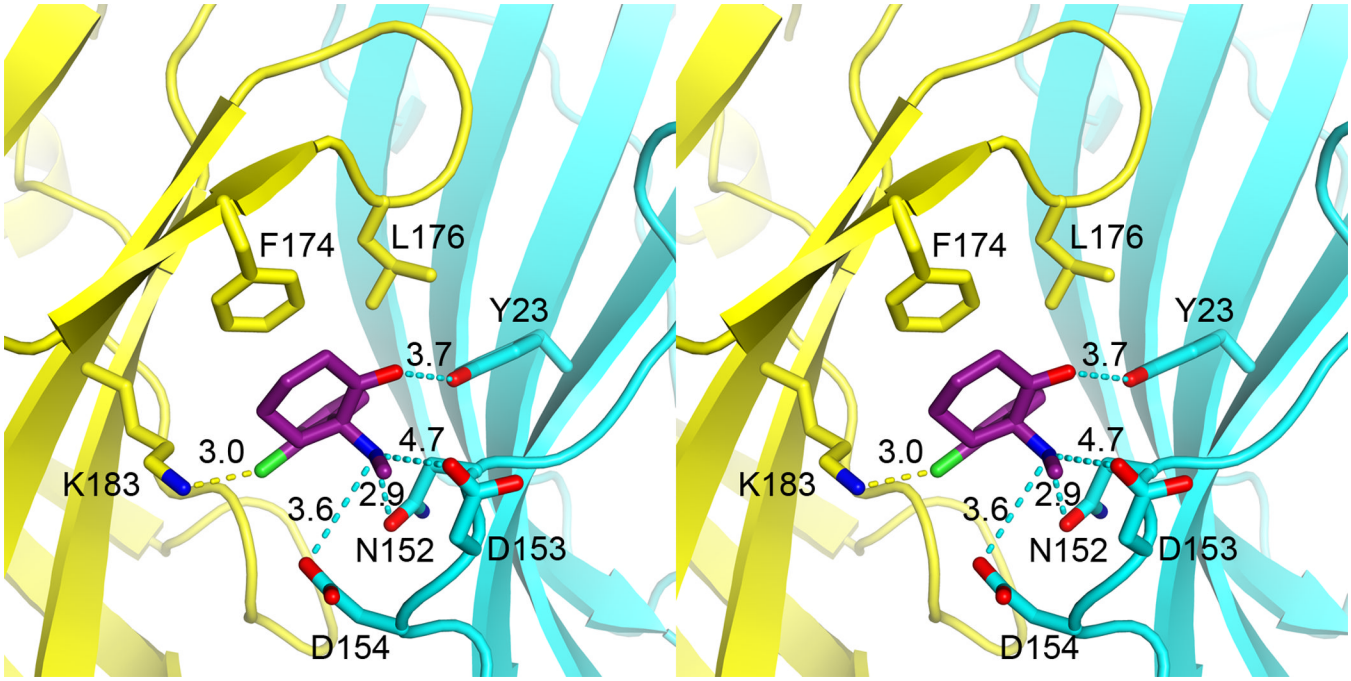

Figure 3. Stereo view of atomic details of the ketamine binding pocket

Dashed lines indicate distances in Å between the ketamine atoms and the relating residues for electrostatic interactions. Residues on the principal and complementary sites of the pocket are colored in yellow and cyan, respectively. Note the position of ketamine relative to N152, in which the mutation affected GLIC activation and ketamine inhibition. See also Figures S3 and S5, and Table S1.

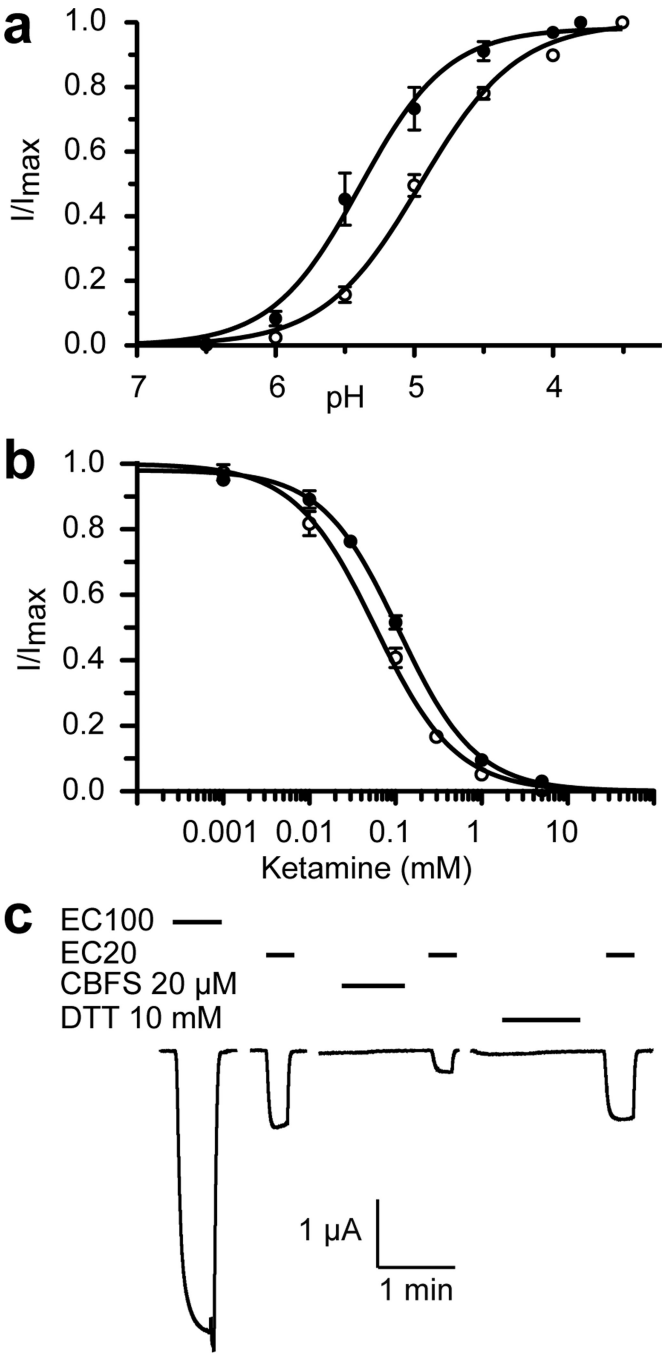

Figure 4. Functional relevance of the ketamine-binding site

(**a**) A single mutation of N152C in the binding pocket altered pH activation of the channel. Currents of the N152C mutant (solid circle) and the wide type GLIC (open circle) expressed in *Xenopus oocytes* were normalized to the maximum current at pH 3.8 or 3.5, respectively. (**b**) The N152C mutation weakened the ketamine inhibition. Responses of the N152 mutant (solid circle) and the wide type GLIC (open circle) are expressed as the fraction of current induced at EC20 in the presence of the indicated concentrations of ketamine relative to that in the absence of ketamine. (**c**) Representative current traces of the N152C_C27A mutant at different pH values, before and after labeling of 8-(chloromercuri)-2-dibenzofuransulfonic

acid (CBFS) at a concentration of 20 μM, and after the treatment of 10-mM dithiothreitol (DTT). The application of CBFS or DTT to *Xenopus oocytes* lasted for ~2 minutes and was followed by the subsequent application of pH 7.4 buffer before a new measurement. The data in (a) and (b) are reported as the mean ± SEM from $n \geq 8$ oocytes and fit to the Hill equation. Error bars less than the symbol size are not visible. See also Figure S4.

Table 1

Data collection and refinement statistics

Data collection and process	
Beamline	SSRL BL 12-2
Wavelength (Å)	0.9795
Space group	C2
Unit cell (Å)	184.1, 132.7, 162.1
β (°)	103.6
Resolution (Å)	25-2.99
R_{merge}(%)[a]	8.3 (59.8)
Completeness (%)[a]	97.6 (92.3)
$<I/\sigma>$[a]	12.6 (2.2)
Unique reflections[a]	74604 (10257)
Redundancy[a]	3.9 (3.9)
Refinement statistics	
Resolution (Å)	24.8-2.99
No. Reflections (test set)	68525 (3452)
R_{work}/R_{feee}	0.187/0.219
Non-H protein (ligand) atoms	13358 (675)
<B-factors> ($Å^2$)	
Protein	70.6
Detergents	125.0
Lipids	119.1
Solvent	51.7
Ketamine	122.3
R.m.s deviations	
Bond lengths (Å)	0.008
Bond angles (degrees)	1.22
Rotamer outliers (%)	8.3
Ramachandran outliers (%)	0.97
Ramachandran favored (%)	93.3
PDB code	4F8H

[a]Values in the parentheses are for highest-resolution shell.